Modeling Char Surface Area Evolution during Coal Pyrolysis: Evolving Characteristics with Coal Rank

He Yang[1], Yahui Yang[1], Sarma V. Pisupati[2], Lijun Jin[1], Yang Li[1], Haoquan Hu[1]*

[1] State Key Laboratory of Fine Chemicals, Institute of Coal Chemical Engineering, School of Chemical Engineering, Dalian University of Technology, Dalian 116024, China

[2] John and Willie Leone Family Department of Energy and Mineral Engineering & EMS Energy Institute, The Pennsylvania State University, 110 Hosler Building, University Park PA 16802 USA

**Corresponding author: hhu@dlut.edu.cn*

Abstract:

Crosslinked metaplast influences char N_2 adsorption specific surface area (S_{N_2}), and the influence changes with coal rank significantly. When crosslinked metaplast is adequate, planar polycyclic aromatic structures overlap tightly and S_{N_2} is small. When crosslinked metaplast content is small, S_{N_2} in crosslinked metaplast is larger than that in the coal matrix and takes a considerable proportion of total char surface area. Two exponents, $k_{\text{mat order}}$ and $k_{\text{crlmet order}}$, representing order degrees of planar polycyclic aromatic structure arrangement in coal matrix and crosslinked metaplast, respectively, were introduced in the previous model for calculating the change of char surface area during coal pyrolysis. The previous model was extended to include predicting S_{N_2} of subbituminous and high-volatile bituminous coals, and was validated

with 5 subbituminous coals, and 2 bituminous coals. The change of S_{N_2} with coal ranks and the transition characteristics between coal ranks can be predicted.

Keywords:

Char Surface Area, Coal Pyrolysis, Coal Rank, Modeling, Metaplast

Introduction

In the numerical simulation for operation optimization of coal conversion processes, various coals usually need to be compared, and therefore, a general char surface area evolution model for different coals is essential.[1-4] However, the change of char specific surface area during coal pyrolysis depends on coal rank very much. Table 1 is the change of char adsorption surface area during the pyrolysis of several lignite and high-volatile bituminous coals (Beulah Zap Lignite, Glen Harold Mine Lignite, Savage Mine Lignite, Pittsburgh #8 Bituminous and Utah Blind Canyon Bituminous).[5-7] When the mass release is less than 30%, the char CO_2 adsorption specific surface area (S_{CO_2}) of lignite coal increase slightly, while that of hv-bituminous char decrease. When the mass release is more than 30%, although the S_{CO_2} of lignite and high-volatile bituminous coal, and char N_2 adsorption surface area (S_{N_2}) of lignite coal changes significantly, the S_{N_2} of the high-volatile bituminous char changes slightly.

The rank of subbituminous coal is between lignite and high-volatile bituminous coals, and the change of S_{N_2} during subbituminous coal pyrolysis exhibits transition characteristics. At 1050 K, during the pyrolysis of New Mexico Blue #1 Subbituminous coal, the change of S_{N_2} is little,

and it is like high-volatile bituminous coal, while at the temperature 1250 K, the S_{N_2} increases from 25 m^2/g to 350 m^2/g rapidly at the mass release 50%, like lignite coal.[5,6] After coal pyrolysis, the chemical composition and polymer network of char is similar for different coals,[5] and the transition characteristics should relate with the metaplast content in char during coal pyrolysis.

Table 1. Change of char adsorption surface area during coal pyrolysis in literature[5-7]

Mass release (daf)	Lignite Char		High-volatile Bituminous Char	
	S_{N_2}	S_{CO_2}	S_{N_2}	S_{CO_2}
0~30%	level off	increase slightly	change slightly (0~25m^2/g)	decrease slightly
30~55%	increase rapidly from 0 to 250 m^2/g	increase rapidly from 200 to 400 m^2/g		increase rapidly from 100 to 300 m^2/g
55~60%	decrease rapidly	level off		level off

It was believed that the metaplast could close the pores in char.[8-10] The metaplast content in char during the pyrolysis of high-volatile bituminous coals is high, making S_{N_2} change little, and even at the end of pyrolysis, after the metaplast is crosslinked with coal matrix and resolidified, S_{N_2} cannot increase. Also, the reduction of S_{CO_2} at the early stage of the pyrolysis of high-volatile bituminous coals should reflect the closing effect of metaplast. It indicates the molten metaplast generated at the early stage of coal pyrolysis can close the pores in char, and this effect can be kept to the late stage of pyrolysis partially. However, as a part of solid char, the crosslinked metaplast cannot be without pores, and actually, the rapid increase of S_{CO_2} at the late stage of the pyrolysis of high-volatile bituminous coals indicates the micropores are increased, but how do the pores adsorbing N_2 are "closed" completely by the solid crosslinked metaplast? In addition,

S_{N_2} of some chars generated at high pressures, which should increase the metaplast content in char by reducing the evaporation, are much larger than that of the chars generated at atmospheric pressure.[11] The effect of metaplast on the char surface area cannot be explained by the "closing effect" completely, and it should relate with the distance between metaplast clusters and the arrangement order.

The thermoplastic phenomena observed in bituminous coals can be described by the space-filling model.[12,13] In this model, planar polycyclic aromatic structures in coal are initially connected and interrupted with each other by the aliphatic bridges. During pyrolysis, the aliphatic bridges are cleaved, and aliphatic radicals diffuse outside to form light gases or attached to the boundary of the aromatic layer. The remaining planar polycyclic aromatic structures, formerly lamellae locked in place by the aliphatic bridges, are free to slide over one another in two dimensions as metaplast to fill the space left by the aliphatic radicals, and the sliding forms the thermoplastic phenomena. After the sliding, the planar polycyclic aromatic structures could be overlapped, and the aromatic clusters can be rearranged in a more orderly and tight fashion. The space-filling model describes a mild evolution process, but the actual reaction and mass transfer during coal pyrolysis are very fast.[14,15] During the thermoplastic deformation, the bubbles in metaplast swell and rupture,[16-18] and it may disturb their arrangements. Before the planar polycyclic aromatic structures are overlapped tightly, it may crosslink with the coal matrix, and the pores between them can be kept in char;[19] meanwhile, the crosslinking bridge may also be cleaved again to release planar polycyclic aromatic structures.

In the previous study, based on the chemical percolation devolatilization (CPD) model,[20-23] a model for the evolution of pore structure in a coal particle during pyrolysis (CPD-PS) was established.[17,24,25] It can predict the experimentally-observed change of S_{N_2} during pyrolysis of

lignite coals and S_{CO_2} during pyrolysis of lignite and high-volatile bituminous coals. In the CPD-PS model, the pore structure in char is assumed to change with the cracking of aliphatic structures. At the early stage of pyrolysis, with the aliphatic bridges and sidechains cleaving, the inside of the char polymer network is opened, and the surface area is increased. Meanwhile, because a significant part of adsorption sites is attached to the aliphatic structures and because the "space-filling" of planar polycyclic aromatic metaplast can make aromatic structures arrange more ordered, at the late stage of pyrolysis., the cleavage of aliphatic structures reduces the adsorption sites in the char and decreases the char surface area. However, for simplification, in the previous model, it was assumed that the adsorption sites in the char reduced linearly with aliphatic structure cleaving. It is reasonable for the adsorption sites attached to the aliphatic structures, but the reduction of the adsorption sites between the planar polycyclic aromatic structures with the aliphatic structure cleaving should not be linear. In addition, the metaplast has more degrees of freedom than the coal matrix, and the movement of metaplast during coal pyrolysis makes the change of adsorption sites in metaplast different from the coal matrix. Especially, because N_2 cannot pass through some small pores that are accessible for CO_2, the effect of metaplast on S_{N_2} is more obvious. The CPD-PS model cannot predict the change of S_{N_2} during the pyrolysis of subbituminous and high-volatile bituminous coals, and the predicted S_{N_2} of lignite coal cannot agree with the experimentally-observed decreasing trend with increasing heating rate.[6]

In this paper, the nonlinear relationship of the adsorption site number in metaplast and between the planar polycyclic aromatic structures with the cleavage of aliphatic structure is analyzed, and the CPD-PS model was improved.

Modeling

In the previous study, the char polymer network parameters and volatile yield calculated by the CPD model were used to calculate char particle structure parameters.[17,24,25] The number of monolayer molecular adsorption sites per aromatic cluster was calculated by Eq. (1), where k_{de} and k_{open} represented the decrease of monolayer molecular adsorption sites and the effect of the pore opening process with aliphatic chain cleaving, respectively; δ^{uncrl} and sp_{g_1} represented the number of side chains and the spaces left by side chain cleaving after considering cross-linking reactions, respectively; M_δ and M_a represented the molecular weight of side chain and adsorbing species, respectively; and σ+1 represented the coordination number, average number of attachments per aromatic cluster.

$$N_{cl}^{ap} = k_{de} \times \frac{sp_{g_1}{}^2(\sigma+1)}{4(\delta^{uncrl}+sp_{g_1})} \times \frac{M_\delta}{M_a} \times k_{open} \quad (1)$$

The change of adsorption sites attached to aromatic and aliphatic structures in the coal matrix and crosslinked metaplast during coal pyrolysis are different. In this paper, N_{cl}^{ap} is divided into the number of monolayer molecular adsorption sites attached to aliphatic structures in coal matrix ($N_{cl\text{-}al\,mat}^{ap}$), the number of monolayer molecular adsorption sites attached to aliphatic structures in crosslinked metaplast ($N_{cl\text{-}al\,crlmet}^{ap}$), the number of monolayer molecular adsorption

sites attached to aromatic structures in coal matrix ($N^{ap}_{\text{cl-ar mat}}$), and the number of monolayer molecular adsorption sites attached to aromatic structures in crosslinked metaplast ($N^{ap}_{\text{cl-ar crlmet}}$).

$N^{ap}_{\text{cl-al mat}}$, $N^{ap}_{\text{cl-al crlmet}}$, $N^{ap}_{\text{cl-ar mat}}$, and $N^{ap}_{\text{cl-ar crlmet}}$ for s_{N_2} and s_{CO_2} are calculated by Eq. (2) - Eq. (6), where f_{cross} and f_{char} represent the weight fraction of crosslinked metaplast and char yield on a dry-ash-free basis of coal. The $f_{\text{cross}} / f_{\text{char}}$ and $1 - f_{\text{cross}} / f_{\text{char}}$ are used to calculate the fractions of crosslinked metaplast and coal matrix in char, respectively, and also, they are used to divide the coal matrix connected with the crosslinked metaplast and that unconnected with the crosslinked metaplast in the calculation of $N^{ap}_{\text{cl-al mat}}$ and $N^{ap}_{\text{cl-ar mat}}$. In the coal matrix connected with the crosslinked metaplast, the k_{de} of the aliphatic structure is set as the average of the k_{de} of aliphatic structure in the coal matrix and the crosslinked metaplast ($(k^{\text{al mat}}_{\text{de}} + k^{\text{al crlmet}}_{\text{de}}) / 2$), and the k_{de} of the aromatic structure is set as the average of the k_{de} of aromatic structure in the coal matrix and the crosslinked metaplast ($(k^{\text{ar mat}}_{\text{de}} + k^{\text{ar crlmet}}_{\text{de}}) / 2$), as shown in Eq. (3) and Eq. (5). The N_2 adsorption specific surface area of the aliphatic structures in coal matrix ($s_{N_2\text{-al mat}}$), the N_2 adsorption specific surface area of aliphatic structures in crosslinked metaplast ($s_{N_2\text{-al crlmet}}$), the N_2 adsorption specific surface area of aromatic structures in coal matrix ($s_{N_2\text{-ar mat}}$), and the N_2 adsorption specific surface area of aromatic structures in crosslinked metaplast ($s_{N_2\text{-ar crlmet}}$) are

calculated by the $N_{\text{cl-sub}}^{\text{ap-N}_2}$ of different structures, respectively. $s_{\text{N}_2\text{-al mat}}$, $s_{\text{N}_2\text{-al crlmet}}$, $s_{\text{N}_2\text{-ar mat}}$, $s_{\text{N}_2\text{-ar crlmet}}$ and $s_{\text{N}_2\text{-particle0}}^{\text{t}}$ (the residual amount of the initial coal particle N_2 adsorption surface area in the char) make up the s_{N_2}.

$$N_{\text{cl}}^{\text{ap}} = N_{\text{cl-al mat}}^{\text{ap}} + N_{\text{cl-al crlmet}}^{\text{ap}} + N_{\text{cl-ar mat}}^{\text{ap}} + N_{\text{cl-ar crmet}}^{\text{ap}} \tag{2}$$

$$N_{\text{cl-al mat}}^{\text{ap}} = (1-\frac{f_{\text{cross}}}{f_{\text{char}}}) \times \left[(1-\frac{f_{\text{cross}}}{f_{\text{char}}}) \times k_{\text{de}}^{\text{al mat}} + \frac{f_{\text{cross}}}{f_{\text{char}}} \times \frac{k_{\text{de}}^{\text{al mat}} + k_{\text{de}}^{\text{al crlmet}}}{2} \right] \times \frac{sp_{\text{g}}{}^{2}(\sigma+1)}{4(\delta^{\text{uncrl}} + sp_{\text{g}_1})} \times \frac{M_{\delta}}{M_{\text{a}}} \times k_{\text{open}}^{\text{al}} \tag{3}$$

$$N_{\text{cl-al crlmet}}^{\text{ap}} = \frac{f_{\text{cross}}}{f_{\text{char}}} \times k_{\text{de}}^{\text{al crlmet}} \times \frac{sp_{\text{g}}{}^{2}(\sigma+1)}{4(\delta^{\text{uncrl}} + sp_{\text{g}_1})} \times \frac{M_{\delta}}{M_{\text{a}}} \times k_{\text{open}}^{\text{al}} \tag{4}$$

$$N_{\text{cl-ar mat}}^{\text{ap}} = (1-\frac{f_{\text{cross}}}{f_{\text{char}}}) \times \left[(1-\frac{f_{\text{cross}}}{f_{\text{char}}}) \times k_{\text{de}}^{\text{ar mat}} + \frac{f_{\text{cross}}}{f_{\text{char}}} \times \frac{k_{\text{de}}^{\text{ar mat}} + k_{\text{de}}^{\text{ar crlmet}}}{2} \right] \times \frac{sp_{\text{g}}{}^{2}(\sigma+1)}{4(\delta^{\text{uncrl}} + sp_{\text{g}_1})} \times \frac{M_{\delta}}{M_{\text{a}}} \times k_{\text{open}}^{\text{ar}} \tag{5}$$

$$N_{\text{cl-ar crlmet}}^{\text{ap}} = \frac{f_{\text{cross}}}{f_{\text{char}}} \times k_{\text{de}}^{\text{ar crlmet}} \times \frac{sp_{\text{g}}{}^{2}(\sigma+1)}{4(\delta^{\text{uncl}} + sp_{\text{g}_1})} \times \frac{M_{\delta}}{M_{\text{a}}} \times k_{\text{open}}^{\text{ar}} \tag{6}$$

A CO_2 molecule can pass through some very small pores and diffuse into spaces that are not accessible by N_2, and only the pores in very deep positions in raw coals initially cannot be reached by CO_2. In the previous study, the aliphatic structure around the aromatic core was assumed as the framework of char surface area, and the "very deep position" for the framework of s_{CO_2} was assumed at the boundary of the aromatic core, while for s_{N_2}, the opening of pores happened around all carbons. In this paper, according to the above physical meaning of pore opening for N_2 and CO_2, the effect of the pore opening process in aromatic structures with aliphatic chain cleaving is calculated by Eq. (7), and that in aliphatic structures for N_2 adsorption specific surface area is calculated by Eq. (8), while for CO_2 adsorption specific surface area it is

set as 1.0 as shown in Eq. (9), where f_a^H, f_a^B, f_a^{sub} and f_{al} represent fractions of protonated, bridgehead, substituent aromatic carbons, and aliphatic carbons, respectively.

$$k_{open}^{ar} = \frac{f_a^{sub} + f_a^B + f_a^H}{f_a^{sub} \times (1 - c_0)} \tag{7}$$

$$k_{open}^{al\text{-}N_2} = \frac{f_{al}}{f_a^{sub} \times (1 - c_0)} \tag{8}$$

$$k_{open}^{al\text{-}CO_2} = 1 \tag{9}$$

In the previous study, k_{de} was set as a linear function of light gas yield. However, k_{de} should be different for different structures. In this paper, it is still assumed that the number of monolayer molecular adsorption sites attached to the aliphatic structures in the coal matrix is decreased linearly with the generation of light gas, and $k_{de}^{al\ mat}$ for N_2 and CO_2 adsorption specific surface area is calculated by Eq. (10), where g_1 represents the amount of light gases generated from the cracking of side chains, g_2 represents the amount of light gases generated along with the formation of char bridge, and c_0 represents the initial fraction of the charred bridges in the raw coal.

$$k_{de}^{al\ mat} = 1 - \frac{g_1 + g_2}{2(1 - c_0)} \tag{10}$$

The number of monolayer molecular adsorption sites attached to the aromatic structures in the coal matrix should decrease with the decreasing fraction of the aliphatic structure in the aromatic clusters, however not linearly. In this work, the adjustable exponent $k_{mat\ order}$ is used to reflect the nonlinear characteristic for the changing amount of N_2 and CO_2 adsorption sites, as shown in Eq. (11). The metaplast is mobile during coal pyrolysis, making the number of

monolayer molecular adsorption sites attached to the structures in crosslinked metaplast decrease with the decreasing aliphatic structure nonlinearly. The adjustable exponents $k_{\text{crlmet order}}$ are added to Eq. (10) and (11) to reflect the nonlinear characteristic of the changing amount of N_2 and CO_2 adsorption sites caused by the metaplast movement, respectively, as shown in Eq. (12) and (13).

$$k_{\text{de}}^{\text{ar mat}} = [M_{\text{al}} k_{\text{de}}^{\text{al mat}} / (M_{\text{ar}} + M_{\text{al}} k_{\text{de}}^{\text{al mat}})]^{k_{\text{mat order}}} \quad (11)$$

$$k_{\text{de}}^{\text{al crlmet}} = (k_{\text{de}}^{\text{al mat}})^{k_{\text{crlmet order}}} \quad (12)$$

$$k_{\text{de}}^{\text{ar crlmet}} = [M_{\text{al}} k_{\text{de}}^{\text{al mat}} / (M_{\text{ar}} + M_{\text{al}} k_{\text{de}}^{\text{al mat}})]^{(k_{\text{mat order}} \times k_{\text{crlmet order}})} \quad (13)$$

$k_{\text{mat order-N}_2}$, $k_{\text{mat order-CO}_2}$, $k_{\text{crlmet order-N}_2}$ and $k_{\text{crlmet order-CO}_2}$ are fitted by the change of char specific surface area during pyrolysis of the Beulah Zap Lignite coal, New Mexico Blue #1 Subbituminous coal, Utah Blind Canyon Bituminous coal, and Pittsburgh #8 Bituminous coal in experiments.[5,6,26] In the fitting, the particle was heated at a heating rate of 5×10^4 K/s to 1300 K and then held at the final temperature for 10 s. The ultimate and proximate analysis of these coals in the fitting and Glen Harold Mine, Savage Mine, Knife River lignite coal, Naomaohu Subbituminous coal, Buliangou Subbituminous coal, Zhundong Subbituminous coal, and Yulin Subbituminous coal reported in literature[5-7,11,27-30] are shown in Table S1 in Supplementary Material for Review, and the fitting results are shown in Figure S1-S4.

The overlap of planar polycyclic aromatic structures is determined by the aliphatic component amount in them, and it is a property of the aromatic structure, so $k_{\text{mat order}}$ should be close for different coals. $k_{\text{crlmet order}}$ should increase with the metaplast content of coal, and therefore, the metaplast content of subbituminous should be bigger than lignite. However,

through data fitting, it is found that $k_{\text{crlmet order-N}_2}$ for Beulah Zap Lignite coal is a little bigger than New Mexico Blue #1 Subbituminous coal, and when $k_{\text{mat order-N}_2}$ is 2.0, $k_{\text{crlmet order-N}_2}$ for Beulah Zap Lignite coal is closest to New Mexico Blue #1 Subbituminous coal, so the $k_{\text{mat order-N}_2}$ is set as 2.0 for all the coals, and then the $k_{\text{crlmet order-N}_2}$ are fitted as 0.5, 0.4, 1.9 and 1.7 for Beulah Zap Lignite coal, New Mexico Blue #1 Subbituminous coal, Pittsburgh #8 Bituminous coal, and Utah Blind Canyon Bituminous coal, respectively. Moreover, the $k_{\text{crlmet order-N}_2}$ of Knife River lignite coal at 0.25 MPa, 0.6 MPa, and 1.0 MPa are fitted by the data in the literature[11] as 0.07, 0.15, and 0.8, respectively. Because of the high metaplast content, the $k_{\text{crlmet order-CO}_2}$ for Pittsburgh #8 Bituminous and Utah Blind Canyon Bituminous coals should not be smaller than 1.0. However, in the fitting in Figure 4 when $k_{\text{mat order-CO}_2}$ is bigger than 0.9, $k_{\text{crlmet order-CO}_2}$ cannot be bigger than 1.0; On the other hand, when $k_{\text{mat order-CO}_2}$ is smaller than 0.5, the calculated s_{CO_2} of Beulah Zap Lignite char is too big and no $k_{\text{crlmet order-CO}_2}$ can fit it, so $k_{\text{mat order-CO}_2}$ is set as 0.7 for all the coals, and then it is found that when $k_{\text{crlmet order-CO}_2}$ is 1.0, the calculated results are good for all the coals.

$k_{\text{mat order-CO}_2}$ (0.7) <1.0, indicates the number of CO_2 adsorption sites attached to the aromatic structures in the coal matrix decreases more slowly than that attached to the aliphatic structures. $k_{\text{mat order-N}_2}$ (2.0) >1.0, indicates the number of N_2 adsorption sites attached to aromatic structures

in coal matrix decreases more rapidly than that attached to aliphatic structures. $k_{\text{crlmet order-CO}_2}$=1.0 indicates the change of the CO_2 adsorption site number in the crosslinked metaplast is the same as that in the coal matrix, and it is different from the molten metaplast. Although in the previous study the molten metaplast can decrease the s_{CO_2},[17] $k_{\text{crlmet order-CO}_2}$=1.0 indicates the CO_2 can pass through the pores between crosslinked metaplast and get the surface area.

$k_{\text{crlmet order-N}_2}$ should relate to the fraction of the crosslinked metaplast (f_{cross}) and the fraction of volatile yield (f_v) in char. The relationship between $k_{\text{crlmet order-N}_2}$ and f_{cross}/f_v is analyzed, as shown in Figure 5. In this figure, for simplification f_{cross}/f_v is set as the value at the end of pyrolysis. At f_{cross}/f_v <0.35, $k_{\text{crlmet order-N}_2}$ is smaller than 1.0 and changes slightly, and it indicates that adequate volatiles pass through the inside structures of coal and keep the planar polycyclic aromatic structures in metaplast arranged disorderly, making the number of N_2 adsorption sites attached to the structures in crosslinked metaplast decreases more slowly than the decrease of aliphatic structures. At f_{cross}/f_v >0.35, $k_{\text{crlmet order-N}_2}$ increases rapidly with the further increase of f_{cross}/f_v, and it indicates that the volatiles are not enough to keep that disorder arrangement and the planar polycyclic aromatic structures in metaplast can slide over one another, making the number of N_2 adsorption sites decreases more rapidly than the decrease aliphatic structures. By fitting the data in Figure 5, Eq. (14) is obtained, and it is used to calculate the change of $k_{\text{crlmet order-N}_2}$ during coal pyrolysis. During coal pyrolysis, f_{cross} and f_v change with mass release, so when Eq. (14) is used in the char surface area model, $k_{\text{crlmet order-N}_2}$ is changed with the changing f_{cross}/f_v.

$$k_{\text{crlmet order-N}_2} = 3.04\times10^{-7}\exp(32.77\times f_{\text{cross}}/f_{\text{v}}) + 0.39 \quad (14)$$

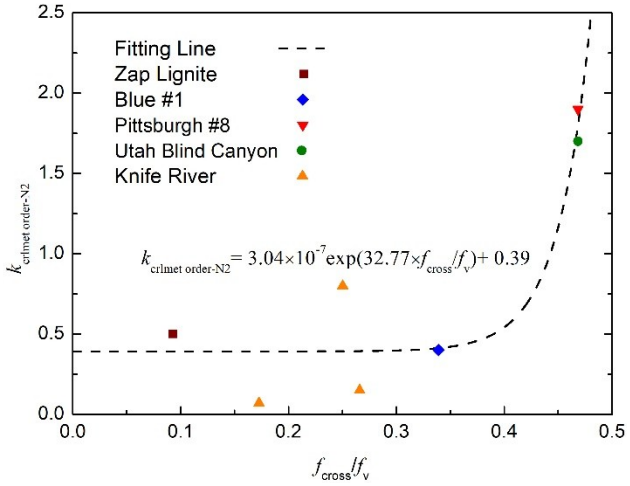

Figure 1. The change of $k_{\text{crlmet order-N}_2}$ with $f_{\text{cross}}/f_{\text{v}}$.

Results and Discussion

The changes of char specific surface area during pyrolysis of 3 lignite coals (Beulah Zap, Glen Harold Mine, and Savage Mine), 5 subbituminous coals (New Mexico Blue #1, Naomaohu, Yulin, Buliangou, Zhundong), and 2 high-volatile bituminous coals (Pittsburgh #8 and Utah Blind Canyon) at different maximum temperatures and heating rates were calculated. The predictions were compared with experimental results to validate the model and analyze the influence of coal rank and heating condition on char specific surface area. Most of these experimental results were from literature.[5-7,26] Moreover, some chars were prepared at the temperatures from 600~1000 ℃ under the nitrogen atmosphere in a drop tube reactor at Dalian University of technology at the heating rate about 1×10^4 K/s, and the specific surface areas of these chars were added in the comparison about the influence of heating rate.

Validation of the model

The predicted and experimental changes in the char surface area of lignite, subbituminous, and high-volatile bituminous coals are compared in Figure 2 - 5. For the lignite coals, high-volatile bituminous coals, and New Mexico Blue #1 Subbituminous coal, whose experimental data were obtained at rapid pyrolysis (heating rate > 1×10^4 K/s),[5-7] in the calculations the particle was heated at a heating rate of 5×10^4 K/s from 300 K to 1300 K, and then held at the final temperature for 10 s. For Zhundong, Naomaohu, Yulin, and Buliangou Subbituminous coals, whose experimental data were obtained at slow pyrolysis (heating rate <1 K/s),[30,31] the heating rate was set as 1 K/s, and after heated to 1300 K the particle was held at the final temperature for 10 s.

The agreement between the predicted changes and experiments in S_{N_2} of lignite coals and the agreement between the predicted changes and experiments in S_{CO_2} of lignite and high-volatile bituminous coals during pyrolysis in the previous study[17,24,25] is still maintained in the improved model (see Figure 2 and 3).

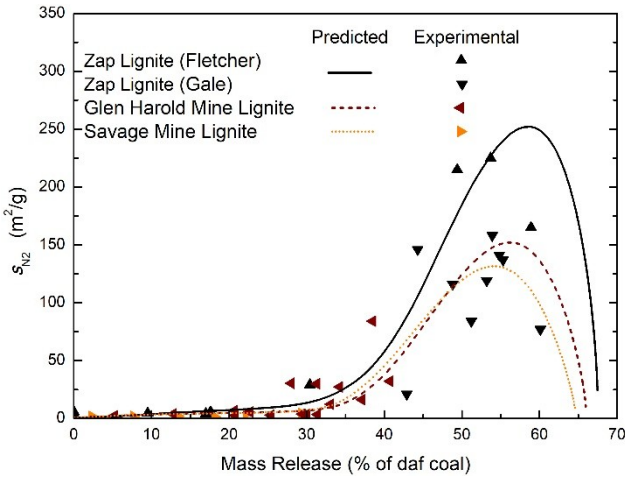

Figure 2. Comparison of the predicted and experimental changes in S_{N_2} of lignite coals during pyrolysis. (Experimental data are from Fletcher et al.[5], Gale et al.[6] and Nsakala et al.[7] Calculation

condition: ambient pressure 0.1 MPa, heating rate 5×10^4 K/s, final temperature 1300 K and residence time 10 s.)

The change in experimental s_{N_2} of high-volatile bituminous coals during pyrolysis is small, and the relative error of the data in Figure 4 is therefore obvious. A first increasing and then decreasing trend can be observed, and the predictions agree with this trend. There are two main peaks in the prediction at the mass release of 47% and 56%, respectively, and between these two peaks, the predicted s_{N_2} fluctuates slightly. The two predicted peaks and fluctuation between them agree with the fluctuation of experimental data at the mass release between 50% and 60%.

The change of s_{N_2} during subbituminous coal pyrolysis is much more complicated than that during the pyrolysis of lignite and high-volatile bituminous coals. There are two kinds of experimental trends in the s_{N_2} of subbituminous coals during pyrolysis in Figure 5. The s_{N_2} of Buliangou coal increases at the mass release of 30%, and this is similar to lignite coals. The s_{N_2} of New Mexico Blue #1 coal and Naomaohu coal change little until the mass release of 50%, which is similar to high-volatile bituminous coals, while at the mass release of 50% the s_{N_2} increases rapidly, and the increase is even larger than lignite char.

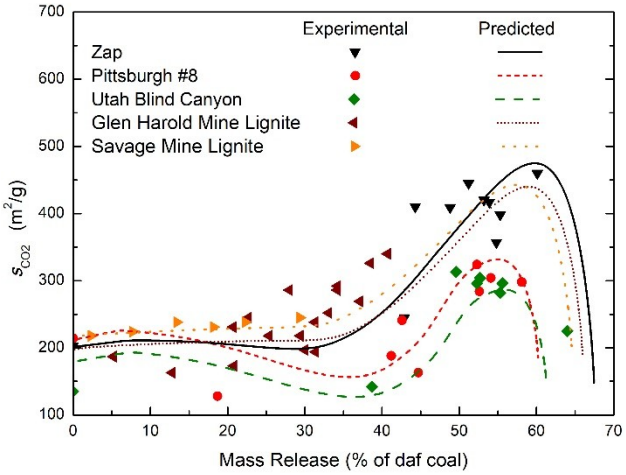

Figure 3. Comparison of the predicted and experimental changes in s_{CO_2} of lignite and bituminous coals during pyrolysis. (Experimental data are from Fletcher et al.[5], Gale et al.[6] and Nsakala et al.[7] Calculation condition: ambient pressure 0.1 MPa, heating rate 5×10^4 K/s, final temperature 1300 K and residence time 10 s.)

The model can reflect the complicated influence of coal rank on the char surface area of subbituminous coal. There are two kinds of predicted curves, the curves with a single peak (Zhundong and Buliangou) and the curves with two peaks (New Mexico Blue #1, Naomaohu, and Yulin). The predicted curves with a single peak start to increase at the mass release of 30%, and the peaks are between the mass release of 40% and 50%. These predicted single peak curves agree with the experimental change in s_{N_2} of Zhundong coal and Buliangou coal, and the predicted trend is close to the predicted changes in s_{N_2} of lignite coals. In the curves with two peaks, the first peak is between the mass release of 35% and 50%, and before the mass release of the second peak, the predicted s_{N_2} is small and close to the change in s_{N_2} of high-volatile bituminous coals. The second predicted peak is at a larger mass release (between 50% and 65%),

and it agrees with the rapid increase of experimental S_{N_2} at the mass release of 50%. The value of the second predicted peak is close to the experimental peak value at the mass release of 50%, and this value is several times as large as the first peak.

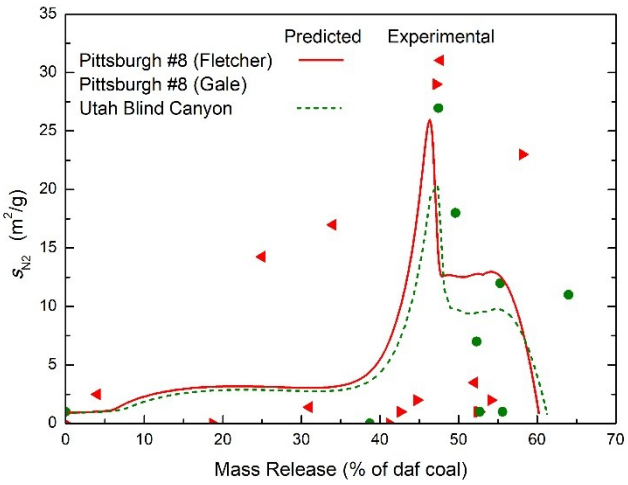

Figure 4. Comparison of the predicted and experimental changes in S_{N_2} of high-volatile bituminous coals during pyrolysis. (Experimental data are from Fletcher et al.[5], and Gale et al.[6] Calculation condition: ambient pressure 0.1 MPa, heating rate 5×10^4 K/s, final temperature 1300 K and residence time 10 s.)

Besides, two points need to be mentioned. (1) the experimental data in Figure 5 were obtained at the temperatures below or equal to1000 °C, and the coal may not be pyrolyzed completely, so the decreasing S_{N_2} at the end of pyrolysis (obtained at the temperatures above to1060 °C) in Figure 2-4 were not observed. However, if the coal pyrolyzed completely, graphitization could decrease the surface area and the predicted decreasing trend of S_{N_2} at the end of pyrolysis should be reasonable. (2) The data of Zhundong, Naomaohu, Yulin, and Buliangou Subbituminous coals in Figure 5 are obtained at slow pyrolysis. However, the CPD

model is not good at predicting slow pyrolysis, and this may influence the accuracy of the prediction.

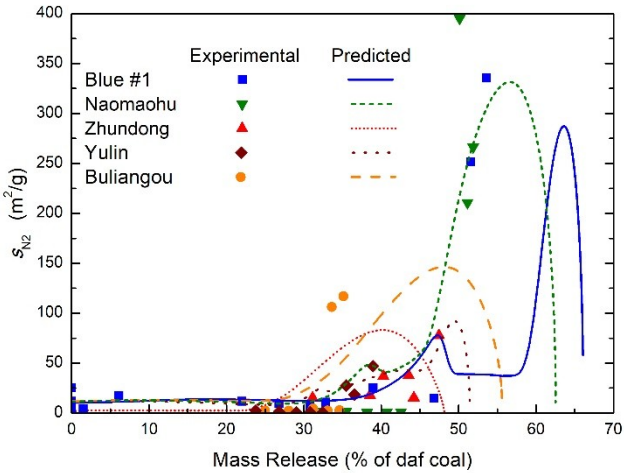

Figure 5. Comparison of the predicted and experimental changes in s_{N_2} of subbituminous coals during pyrolysis. (Experimental data are from Fletcher et al.,[5,6] Zhang et al.,[31] and Yang et al.[30] Calculation condition: ambient pressure 0.1 MPa, heating rate 5×10^4 K/s for New Mexico Blue #1 and 1 K/s for other coals, final temperature 1300 K, and residence time 10 s for New Mexico Blue #1 and 1010 s for other coals.)

Influence of coal rank

The predicted distributions of s_{N_2} in different structures in char during pyrolysis of Zap Lignite coal, Pittsburgh #8 Bituminous coal, New Mexico Blue #1 Subbituminous coal are shown in Figure 6, 8, and 10, respectively, while correspondingly the predicted changes of $k_{\text{crln et order-N}_2}$, f_{gas}, f_{tar}, f_{cross} and $f_{\text{cross}}/f_{\text{v}}$ are shown in Figure 7, 9 and 11. In the calculation, the particle was heated at a heating rate of 5×10^4 K/s from 300 K to 1300 K and then held at the final temperature for 10 s.

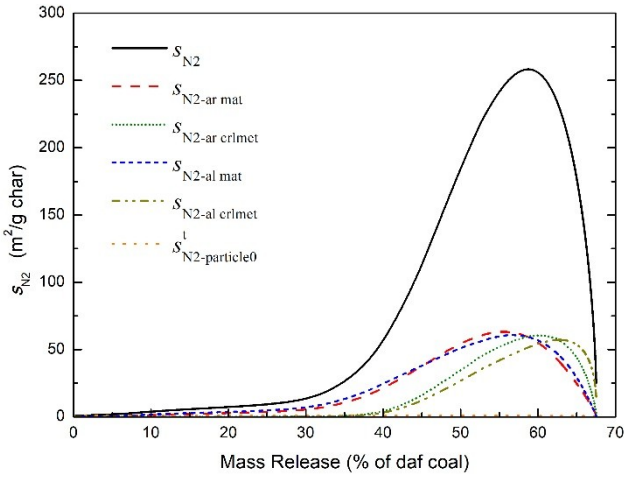

Figure 6. The predicted distributions of s_{N_2} during Zap Lignite coal pyrolysis. (Calculation condition: heating rate 5×10^4 K/s, final temperature 1300 K and residence time 10 s.)

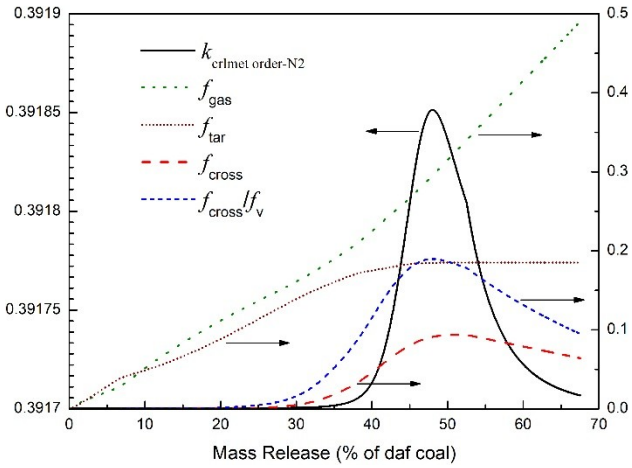

Figure 7. The predicted change of $k_{\text{crlmet order-N}_2}$, f_{gas}, f_{tar}, f_{cross} and f_{cross}/f_v during Zap Lignite coal pyrolysis. (Calculation condition: heating rate 5×10^4 K/s, final temperature 1300 K and residence time 10 s.)

During pyrolysis of Zap Lignite coal, lesser crosslinked metaplast forms, while a lot of gas and tar generate, and $k_{\text{crlmet order-N}_2}$ keeps at a small value (see Figure 7), making the crosslinked metaplast arranged very disorderly. Therefore, the specific surface area of the aliphatic and

aromatic structures in the crosslinked metaplast is big, and although the content of crosslinked metaplast is small, its surface area takes a considerable proportion of the total char surface area.

During the pyrolysis of Pittsburgh #8 Bituminous coal, much more crosslinked metaplast forms, and the volatile yield is lesser. $k_{\text{crlmet order-N}_2}$ can increase to a very high value (see Figure 9), and even at the end of pyrolysis $k_{\text{crlmet order-N}_2}$ is still bigger than 1. With the bigger $k_{\text{crlmet order-N}_2}$, the planar polycyclic aromatic structures can be overlapped tightly, and therefore, the specific surface area of the aliphatic and aromatic structures in the crosslinked metaplast is small. With the generation of volatiles, the crosslinked metaplast becomes the main part of char, and the char surface area is restrained at a small value.

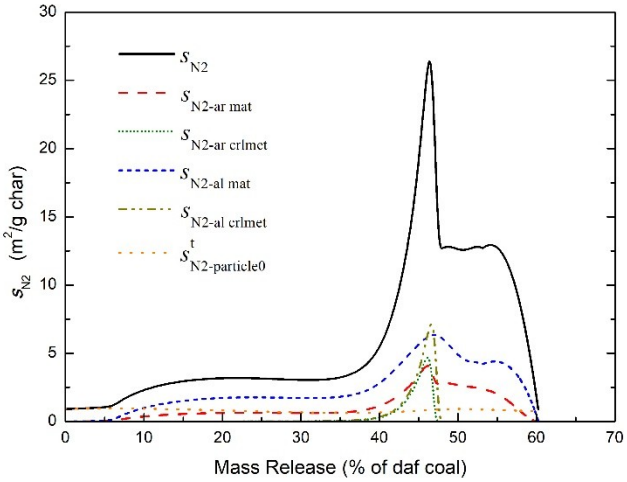

Figure 8. The predicted distributions of S_{N_2} during Pittsburgh #8 Bituminous coal pyrolysis. (Calculation condition: heating rate 5×10^4 K/s, final temperature 1300 K and residence time 10 s.)

During the pyrolysis of New Mexico Blue #1 Subbituminous coal, the content of metaplast is bigger than Zap Lignite coal and smaller than Pittsburgh #8 Bituminous coal. When the mass

release is between 45% and 60%, $k_{\text{crlmet order-N}_2}$ is bigger than 1, and the char surface area is restrained at a small value, similar to high-volatile bituminous coals. However, at the late stage of pyrolysis, $k_{\text{crlmet order-N}_2}$ become smaller than 1, making the specific surface area of the aliphatic and aromatic structures in the crosslinked metaplast increase, and the second peak of s_{N_2} is formed.

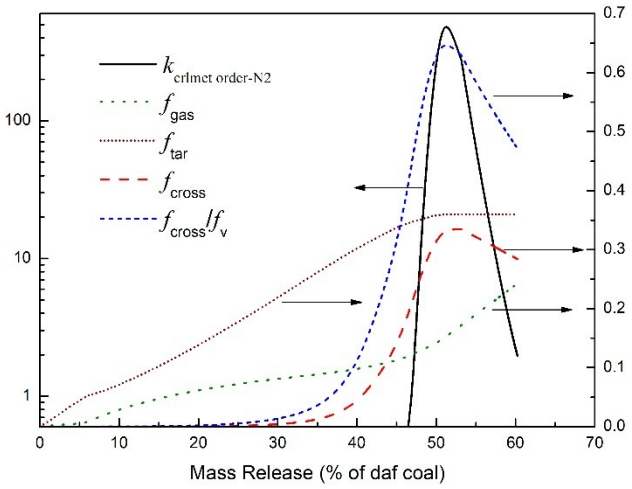

Figure 9. The predicted change of $k_{\text{crlmet order-N}_2}$, f_{gas}, f_{tar}, f_{cross} and $f_{\text{cross}}/f_{\text{v}}$ during Pittsburgh #8 Bituminous coal pyrolysis. (Calculation condition: heating rate 5×10^4 K/s, final temperature 1300 K and residence time 10 s.)

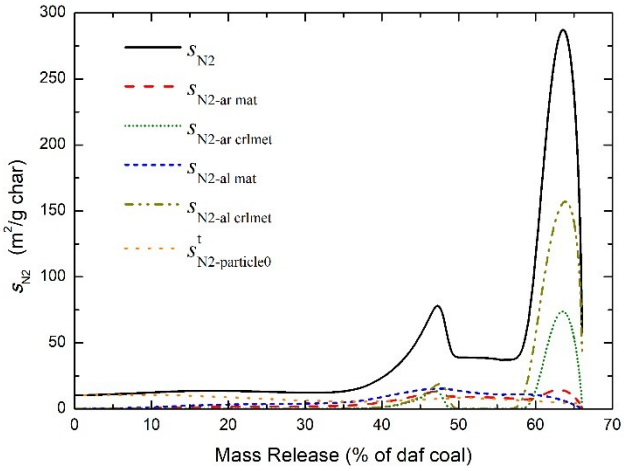

Figure 10. The predicted distributions of s_{N_2} during New Mexico Blue #1 Subbituminous coal pyrolysis. (Calculation condition: heating rate 5×10^4 K/s, final temperature 1300 K and residence time 10 s.)

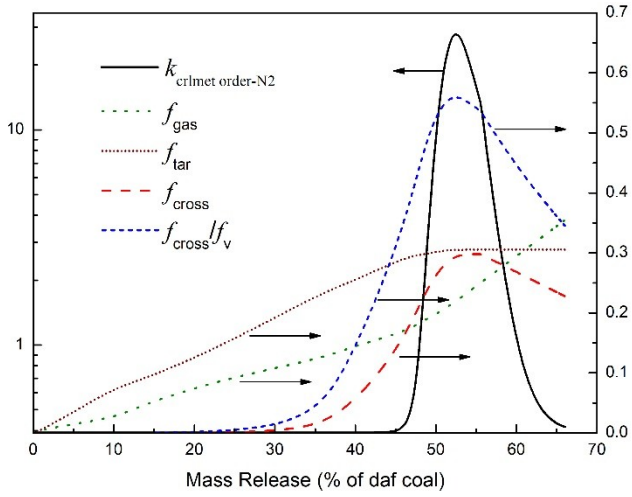

Figure 11. The predicted change of $k_{crlmet\ order\text{-}N_2}$, f_{gas}, f_{tar}, f_{cross} and f_{cross}/f_v during New Mexico Blue #1 Subbituminous coal pyrolysis. (Calculation condition: heating rate 5×10^4 K/s, final temperature 1300 K and residence time 10 s.)

The changes of s_{N_2} with different ranks are controlled by $k_{crlmet\ order\text{-}N_2}$. The predicted change of s_{N_2} with different $k_{crlmet\ order\text{-}N_2}$ during pyrolysis of Pittsburgh #8 Bituminous coal and New

Mexico Blue #1 Subbituminous coal is shown in Figure 12. When $k_{\text{crlmet order-N}_2}$ =10, the predicted s_{N_2} is small. When $k_{\text{crlmet order-N}_2}$ =0.4, the predicted change of s_{N_2} is a curve with one single peak, and the predicted s_{N_2} of lignite coal in Figure 6 is this kind of curve. When $k_{\text{crlmet order-N}_2}$ is set as the function of f_{cross}/f_v, the predicted s_{N_2} is between the curves of $k_{\text{crlmet order-N}_2}$ =10 and $k_{\text{crlmet order-N}_2}$ =0.4: before the metaplast is crosslinked, $k_{\text{crlmet order-N}_2}$ is small, and the s_{N_2} of Pittsburgh #8 Bituminous coal and New Mexico Blue #1 Subbituminous coal are both increased along with the curve with one single peak; then with the increasing crosslinked metaplast $k_{\text{crlmet order-N}_2}$ is increased, and the predicted s_{N_2} changes along with the curve of $k_{\text{crlmet order-N}_2}$ =10; at the end of pyrolysis, the $k_{\text{crlmet order-N}_2}$ of New Mexico Blue #1 Subbituminous coal can decrease to a small value, the predicted s_{N_2} will increase to the curve with one single peak again, and changes further along with this curve.

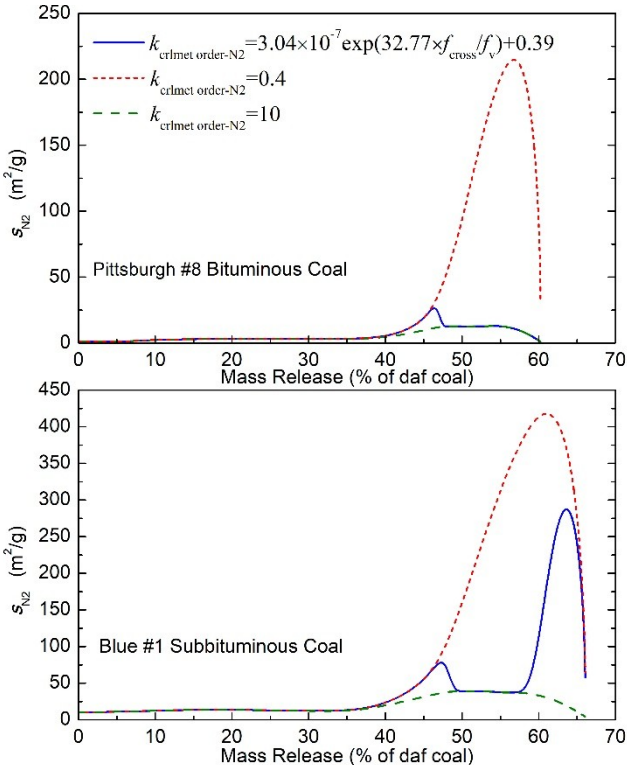

Figure 12. Comparison of the predicted change of s_{N_2} with different $k_{crlmet\ order\text{-}N_2}$ during Pittsburgh #8 Bituminous coal and New Mexico Blue #1 Subbituminous coal pyrolysis. (Calculation condition: heating rate 5×10^4 K/s, final temperature 1300 K and residence time 10 s.)

The change of $k_{crlmet\ order\text{-}N_2}$ during coal pyrolysis is complicated, and it may be influenced by many factors, such as particle fragmentation, plastic deformation, free radical exchange, volatile secondary reaction, and gasification reaction. However, the introduction of $k_{crlmet\ order\text{-}N_2}$ as the function of f_{cross}/f_v makes the model be able to reflect the influence of coal rank on s_{N_2}. The predicted changes of $k_{crlmet\ order\text{-}N_2}$ for the pyrolysis of subbituminous coals in Figure 5 are shown

in Figure 13. The $k_{\text{crlmet order-N}_2}$ of Buliangou and Zhundong coals is small, and therefore, correspondingly the predicted change of s_{N_2} is more like lignite coal. The predicted $k_{\text{crlmet order-N}_2}$ of New Mexico Blue #1 coal and Naomaohu coal change largely, and therefore, correspondingly the predicted changes of s_{N_2} are cures with two peaks. The predicted $k_{\text{crlmet order-N}_2}$ of Yulin coal is even large enough to be close to high-volatile bituminous coals, and the predicted changes of s_{N_2} is small and similar to char of high-volatile bituminous coals.

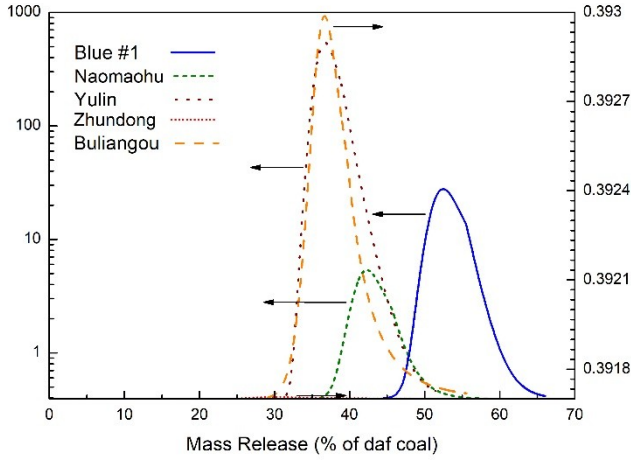

Figure 13. The predicted change of $k_{\text{crlmet order-N}_2}$ during pyrolysis of subbituminous coals. (Calculation condition: ambient pressure 0.1 MPa, heating rate 5×10^4 K/s for New Mexico Blue #1 and 1 K/s for other coals, final temperature 1300 K, and residence time 10 s for New Mexico Blue #1 and 1010 s for other coals.)

Influence of maximum temperature

The predicted changes of s_{N_2} during the pyrolysis of New Mexico Blue #1 Subbituminous coal at different maximum temperatures are shown in Figure 14. In the calculation, the particle was heated at a heating rate of 5×10^4 K/s from 300 K to different final temperatures and then

held at the final temperature for 10 s. A higher temperature can increase the vaporization of metaplast, more bridges and side chains can also crack to generate light gases, and therefore, at a higher temperature, $k_{\text{crlmet order-N}_2}$ is smaller. At a lower temperature (1000 K in Figure 14), the side chains tightly connected with aromatic carbon cannot crack, making $k_{\text{crlmet order-N}_2}$ much larger than 1.0 at the end of pyrolysis, and there is not the second peak in the curve of the predicted s_{N_2}. At the temperatures high enough (≥1100 K in Figure 14), the side chains tightly connected with aromatic carbon will be cleaved, and the light gases generated from these side chains will decrease $k_{\text{crlmet order-N}_2}$ to the value under 1.0 at the end of pyrolysis, forming the second peak of s_{N_2} curve.

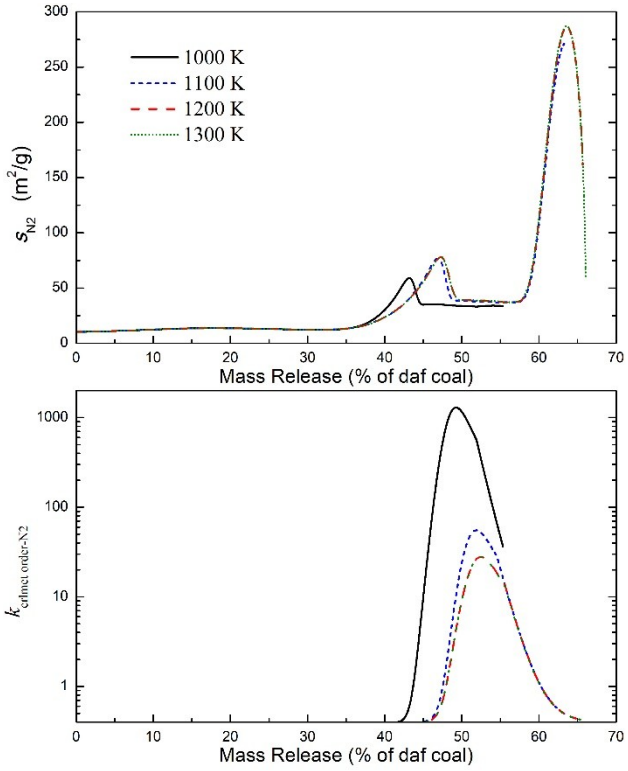

Figure 14. The predicted changes of s_{N_2} and $k_{\text{crlmet order-}N_2}$ of New Mexico Blue #1 Subbituminous coal during pyrolysis at different maximum temperatures. (Calculation condition: ambient pressure 0.1 MPa, heating rate 5×10^4 K/s, and residence time 10 s.)

The model can support the experimentally-observed dependence of s_{N_2} with temperature during New Mexico Blue #1 Subbituminous coal pyrolysis,[5,6] as shown in Figure 15. The predicted s_{N_2} keeps in the value under 70 m^2/g at 1050 K, while the maximum predicted s_{N_2} increases to 300 m^2/g at 1250 K, and this agrees with the experimental trend. If the change of $k_{\text{crlmet order-}N_2}$ during coal pyrolysis is not considered (setting $k_{\text{crlmet order-}N_2}$ =0.4), the predicted s_{N_2} can increase very high at the temperature 1050 K, and it does not agree with the experimental results.

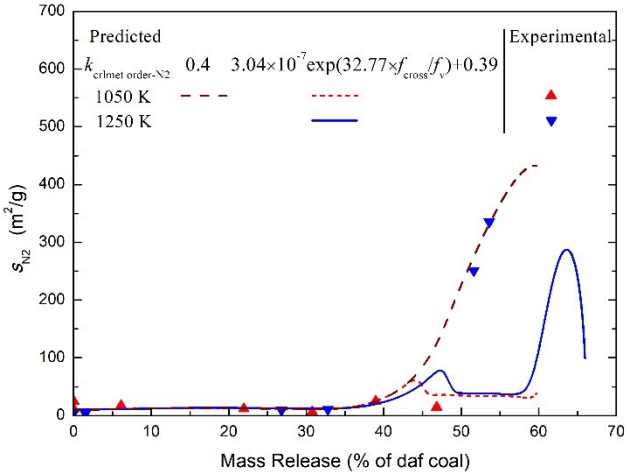

Figure 15. Comparison of the predicted and experimental changes in s_{N_2} of New Mexico Blue #1 Subbituminous coal during pyrolysis at different maximum temperatures. (Experimental data are from Fletcher et al.[5,6] Calculation condition: ambient pressure 0.1 MPa, heating rate 5×10^4 K/s, and residence time 10 s.)

Influence of heating rate

The predicted changes of S_{N_2} during the pyrolysis of Zap Lignite coal, Pittsburgh #8 Bituminous coal, New Mexico Blue #1 Subbituminous coal, and Naomaohu Subbituminous coal are shown in Figure 16, 17, 18, and 19, respectively. In the calculation, the particle was heated from 300 K to 1300 K at different heating rates and then held at the final temperature for 10 s.

The S_{N_2} of these chars prepared in the rapid pyrolysis with the drop tube reactor at Dalian University of technology and chars generated in the slow pyrolysis from literature[30] are compared with the prediction in Figure 19.

The changes of S_{N_2} during the pyrolysis of different coals are different. The maximum predicted S_{N_2} of Zap Lignite coal and Naomaohu Subbituminous coal decreases with increasing heating rate, while that of Pittsburgh #8 Bituminous coal and New Mexico Blue #1 Subbituminous coal increases with increasing heating rate.

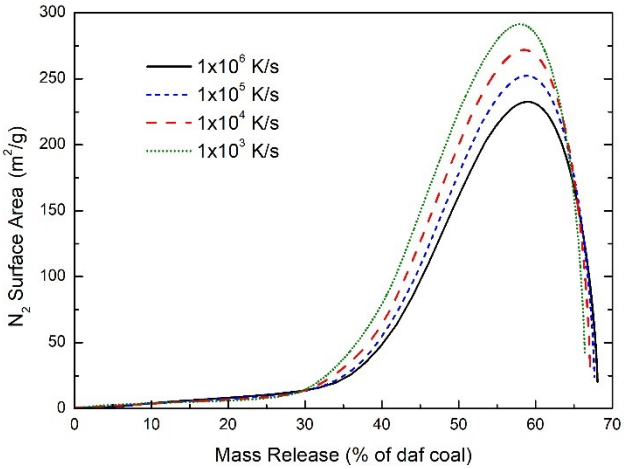

Figure 16. The predicted changes of S_{N_2} during Zap Lignite coal pyrolysis at different heating rates. (Calculation condition: ambient pressure 0.1 MPa and final temperature 1300 K.)

A higher heating rate can make the char reach a higher temperature earlier, and improve the vaporization of metaplast, making $k_{\text{crlmet order-N}_2}$ increase with decreasing heating rate as shown in Figure 20. With a smaller $k_{\text{crlmet order-N}_2}$ at a higher heating rate, the s_{N_2} should be larger. However, the s_{N_2} is also influenced by the content of crosslinked metaplast in char. The changes of s_{N_2} at different heating rates with the $k_{\text{crlmet order-N}_2}$ set as different constant (0.4 and 10) are compared in Figure 21. When $k_{\text{crlmet order-N}_2}$ <1.0, the specific surface area of crosslinked metaplast is larger than the coal matrix, and with more vaporization of metaplast, the s_{N_2} is decreased with increasing heating rate; and when $k_{\text{crlmet order-N}_2}$ >1.0, the specific surface area of crosslinked metaplast is smaller than the coal matrix, and the more vaporization of metaplast makes s_{N_2} increase with increasing heating rate.

During pyrolysis of Zap Lignite coal, $k_{\text{crlmet order-N}_2}$ keeps in a small value as shown in Figure 7. Therefore, the maximum predicted s_{N_2} decreases with increasing heating rates (see Figure 16), and it agrees with the experiments in the literature.[6] In addition, with more metaplast evaporated at the early stage of pyrolysis, the peak moves to the higher mass release.

During the pyrolysis of Naomaohu Subbituminous coal, at the heating rate 1K/s, $k_{\text{crlmet order-N}_2}$ can be bigger than 1.0 as shown in Figure 13. However, the duration is short and $k_{\text{crlmet order-N}_2}$ is

decreased with increasing heating rate. At the heating rate 100 K/s, the curve of s_{N_2} changes from the curve with two peaks to the curve with one single peak, and then the curve varies with increasing heating rates like lignite coal. The maximum predicted s_{N_2} decreases and the peak moves to the higher mass release with increasing heating rates, which agrees with the experiments (see Figure 19).

In addition, with more vaporization of metaplast at a higher heating rate, $k_{\text{crlmet order-}N_2}$ decrease at the late stage of pyrolysis, and the second peak of the s_{N_2} curve becomes larger and starts to increase earlier as shown in Figure 18. Even during the pyrolysis of Pittsburgh #8 Bituminous coal, at a very high heating rate (1×10^6 K/s in Figure 17), when $k_{\text{crlmet order-}N_2}$ is small enough, the second peak become bigger than the first one, which agrees with the fluctuation of experimental data at the mass release between 55% and 60% in Figure 4. Meanwhile, at a very low heating rate (100 K/s in Figure 16), when $k_{\text{crlmet order-}N_2}$ is big enough, the increase of s_{N_2} of New Mexico Blue #1 Subbituminous coal at the mass release between 45% and 55% is restrained completely, and the second peak of s_{N_2} curve become unapparent, more like the curves of high-volatile bituminous coals, as shown in Figure 8.

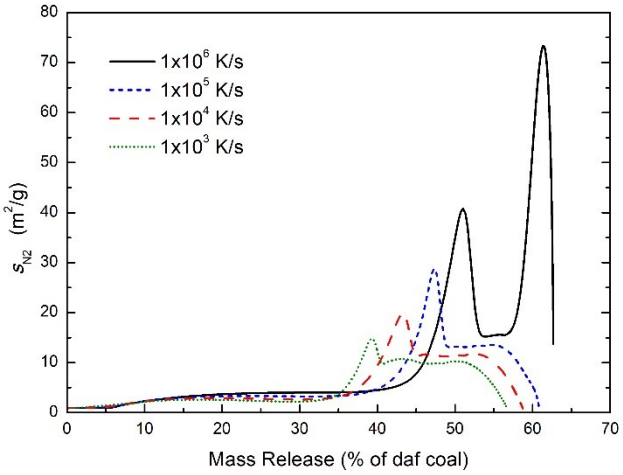

Figure 17. The predicted changes of s_{N_2} during Pittsburgh #8 Bituminous coal pyrolysis at different heating rates. (Calculation condition: ambient pressure 0.1 MPa and final temperature 1300 K.)

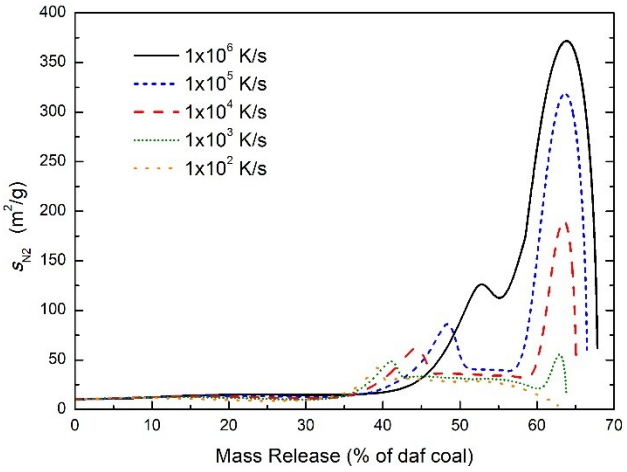

Figure 18. The predicted changes of s_{N_2} during New Mexico Blue #1 Subbituminous coal pyrolysis at different heating rates. (Calculation condition: ambient pressure 0.1 MPa and final temperature 1300 K.)

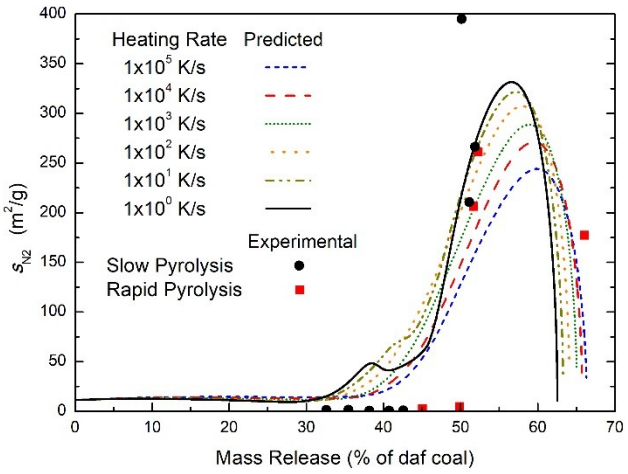

Figure 19. Comparison of the predicted and experimental changes in s_{N_2} during Naomaohu Subbituminous coal pyrolysis at different heating rates. (The circle symbols are from literature[30]; and the square symbols are the surface area of char prepared in this work. Calculation condition: ambient pressure 0.1 MPa and final temperature 1300 K.)

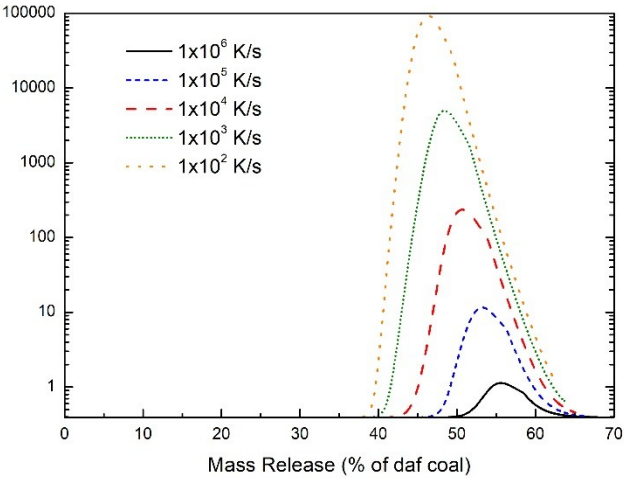

Figure 20. The predicted changes of $k_{\text{crlmet order-}N_2}$ during New Mexico Blue #1 Subbituminous coal pyrolysis at different heating rates. (Calculation condition: ambient pressure 0.1 MPa and final temperature 1300 K.)

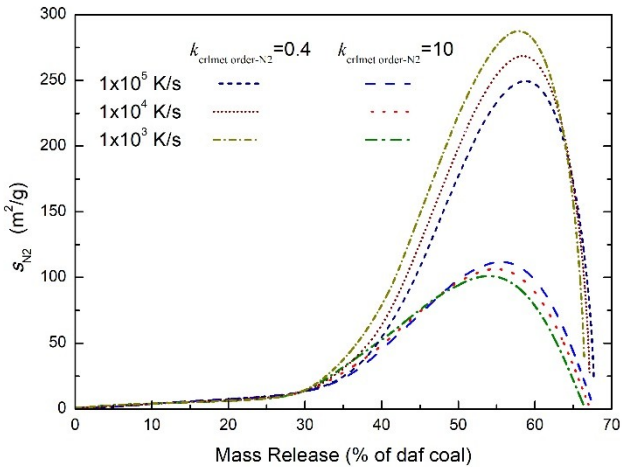

Figure 21. The predicted changes of $k_{crlmet\ order\text{-}N_2}$ during Zap Lignite coal pyrolysis at different heating rates and different $k_{crlmet\ order\text{-}N_2}$. (Calculation condition: ambient pressure 0.1 MPa and final temperature 1300 K.)

Conclusions

The effect of the order degree of planar polycyclic aromatic structure arrangement on char surface area was analyzed, and two exponents, $k_{mat\ order}$ and $k_{crlmet\ order}$, representing the order degrees of planar polycyclic aromatic structure arrangement in the coal matrix and metaplast respectively, were introduced in the previous CPD-PS model. A correlation between the $k_{crlmet\ order\text{-}N_2}$ and f_{cross}/f_v was fitted, and the $k_{mat\ order\text{-}CO_2}$, $k_{crlmet\ order\text{-}CO_2}$ and $k_{mat\ order\text{-}N_2}$ were set as 0.7, 1.0, and 2.0, respectively. The application of the CPD-PS model, which could predict s_{N_2} of lignite coals and s_{CO_2} of lignite and high-volatile bituminous coals during pyrolysis, was extended to include s_{N_2} of subbituminous and high-volatile bituminous coals.

The trend of changing s_{N_2} during coal pyrolysis was determined by f_{cross}/f_v, and it is reflected by $k_{crlmetorder\text{-}N_2}$. During pyrolysis of lignite coals and some subbituminous coals with lesser metaplast (Buliangou coal and Zhundong coal), with $k_{crlmetorder\text{-}N_2}$ keeping at a small value (<0.4), the crosslinked metaplast arranges disorderly, s_{N_2} first increases and then decreases, and the maximum s_{N_2} could be more than 250 m^2/g. During pyrolysis of high-volatile bituminous coals and some subbituminous coals with adequate metaplast (Yulin coal) at the heating rate $\leq 1\times10^5$ K/s, $k_{crlmetorder\text{-}N_2}$ keeps at a value bigger than 1.0, and the planar polycyclic aromatic structures overlap tightly to restrain s_{N_2} at a small value. The changes of s_{N_2} during pyrolysis of New Mexico Blue #1 Subbituminous coal and Naomaohu Subbituminous coal are curves with two stages: at the early stage, $k_{crlmetorder\text{-}N_2}$ is bigger than 1.0, making s_{N_2} change little like high-volatile bituminous coals; and at the late stage $k_{crlmetorder\text{-}N_2}$ decreases to the value smaller than 1.0, making s_{N_2} increase rapidly and then further change like lignite coals.

The maximum temperature determines the maximum mass release during coal pyrolysis. During New Mexico Blue #1 coal pyrolysis, at the maximum temperature < 1100 K, $k_{crlmetorder\text{-}N_2}$ keeps at the value bigger than 1.0, restraining s_{N_2} at a small value, like high-volatile bituminous

coals; and at the maximum temperature > 1100 K, $k_{\text{crlmet order-N}_2}$ can decrease to the value smaller than 1.0, making s_{N_2} first increase and then decrease rapidly at the end of pyrolysis.

The increase in heating rate can improve the vaporization of metaplast and decrease $k_{\text{crlmet order-N}_2}$. During pyrolysis of lignite coals and some subbituminous coals with lesser metaplast, because $k_{\text{crlmet order-N}_2}$ is kept smaller than 1.0, the N_2 adsorption specific surface area of structures in crosslinked metaplast is larger than that in coal matrix, and therefore, the increased vaporization of metaplast at a higher heating rate decreases s_{N_2} and moves the s_{N_2} peak to the higher mass release. During pyrolysis of bituminous coals and some subbituminous coals with more metaplast, $k_{\text{crlmet order-N}_2}$ can be bigger than 1.0, and at a higher heating rate, s_{N_2} increases with decreasing $k_{\text{crlmet order-N}_2}$ and increasing vaporization of metaplast. At a very high heating rate (>1×10^6 K/s), when $k_{\text{crlmet order-N}_2}$ is decreased adequately, even the s_{N_2} of Pittsburgh #8 Bituminous coal can sharply increase and then decrease at the end of pyrolysis, similar to New Mexico Blue #1 coal at the heating of 5×10^4 K/s. At a low heating rate (<100 K/s), when $k_{\text{crlmet order-N}_2}$ is big enough, during New Mexico Blue #1 coal pyrolysis the second peak of s_{N_2} curve becomes unapparent, more like the curves of high-volatile bituminous coals at the heating of 5×10^4 K/s.

Acknowledgments

This work is supported by the National Key Research and Development Program of China (2016YFB0600301), the National Science Foundation for Young Scholars of China (21706025), the Fundamental Research Funds for the Central Universities (DUT2018TB02), and China Scholarship Council (CSC, 201806065065).

References

1. Yan BH, Cheng Y, Xu PC, Cao CX, Cheng Y. Generalized model of heat transfer and volatiles evolution inside particles for coal devolatilization. *AIChE Journal.* 2014;60(8):2893-2906.

2. Gavalas GR, Wilks KA. Intraparticle mass-transfer in coal pyrolysis. *AIChE Journal.* 1980;26(2):201-212.

3. Shen ZJ, Xu JL, Liu HF, Liang QF. Modeling study for the effect of particle size on char gasification with CO_2. *AIChE Journal.* 2017;63(2):716-724.

4. Li F-z, Feng J, Li X-h, Li W-y, Wang J. A model of devolatilization behavior in lignite pyrolysis with solid heat carriers. *AIChE Journal.* Jun 2019;65(6).

5. Fletcher TH, Hardesty DR. *Compilation of Sandia coal devolatilization data: Milestone report.* Livermore, CA, USA: Sandia National Laboratories;1992. SAND92-8209.

6. Gale TK, Fletcher TH, Bartholomew CH. Effects of pyrolysis conditions on internal surface areas and densities of coal chars prepared at high heating rates in reactive and non-reactive atmospheres. *Energy Fuels.* 1995;9:513-524.

7. Nsakala NY, Essenhigh RH, Walker PL. Characteristics of chars produced from lignites by pyrolysis at 808°c following rapid heating. *Fuel.* 1978;57:605-611.

8. Yu J, Strezov V, Lucas J, Wall T. Swelling behaviour of individual coal particles in the single particle reactor. *Fuel.* 2003; 82(16):1977-1987.

9. Sheng S, Azevedo JLT. Modeling the evolution of particle morphology during coal devolatilization. *Proceedings of the Combustion Institute.* 2000;28:2225–2232.

10. Oh MS, Peters WA, Howard JB. An experimental and modeling study of softening coal pyrolysis. *AIChE Journal.* 1989;35(5):775-792.

11. Zeng D, Fletcher TH. Effects of pressure on coal pyrolysis and char morphology. *Energy Fuels.* Sep-Oct 2005;19(5):1828-1838.

12. Spiro CL. SPACE-FILLING MODELS FOR COAL - A MOLECULAR DESCRIPTION OF COAL PLASTICITY. *Fuel.* 1981;60(12):1121-1126.

13. Spiro CL, Kosky PG. SPACE-FILLING MODELS FOR COAL .2. EXTENSION TO COALS OF VARIOUS RANKS. *Fuel.* 1982;61(11):1080-&.

14. Bliek A, Vanpoelje WM, Vanswaaij WPM, Vanbeckum FPH. Effects of intraparticle heat and mass-transfer during devolatilization of a single coal particle. *AIChE Journal.* 1985;31(10):1666-1681.

15. Yang H, Li SF, Fletcher TH, Dong M, Zhou WS. Simulation of the evolution of pressure in a lignite particle during pyrolysis. *Energy & Fuels.* 2014;28(5):3511-3518.

16. Yang H, Li S, Fletcher TH, Dong M. Simulation of the swelling of high-volatile bituminous coal during pyrolysis. *Energy Fuels.* 2014;28(11):7216–7226.

17. Yang H, Fletcher TH, Li S, Hu H, Jin L, Li Y. Model for the evolution of pore structure in a lignite particle during pyrolysis. 2.Iinfluence of cross-linking reactions, molten metaplast, and molten ash on particle surface area. *Energy & Fuels.* 2017;31:8036-8044.

18. Yu J, Lucas J, Wall. T. Modeling the development of char structure during the rapid heating of pulverized coal. *Combustion and Flame.* 2004;136:519-532.

19. de la Puente G, Marban G, Fuente E, Pis JJ. Modelling of volatile product evolution in coal pyrolysis. The role of aerial oxidation. *Journal of Analytical and Applied Pyrolysis.* Jan 1998;44(2):205-218.

20. Fletcher TH. Review of 30 years of research using the Chemical Percolation Devolatilization Model. *Energy & Fuels.* Dec 2019;33(12):12123-12153.

21. Grant DM, Pugmire RJ, Fletcher TH, Kerstein AR. Chemical model of coal devolatilization using percolation lattice statistics. *Energy Fuels.* 1989;3:175-186.

22. Fletcher TH, Kerstein AR, Pugmire RJ, Grant DM. Chemical percolation model for devolatilization. 2. Temperature and heating rate effects on product yields. *Energy Fuels.* 1990;4:54-60.

23. Fletcher TH, Kerstein AR, Pugmire RJ, Solum MS, Grant DM. Chemical percolation model for devolatilization. 3. Direct use of ^{13}C NMR data to predict effects of coal type. *Energy Fuels.* 1992;6(4):414-431.

24. Yang H, Fletcher TH, Li Y, et al. Modeling the influence of changes in aliphatic structure on char surface area during coal pyrolysis. *AIChE J.* 2019;66(2):DOI: 10.1002/aic.16834.

25. Li SF, Yang H, Fletcher TH, Dong M. Model for the evolution of pore structure in a lignite particle during pyrolysis. *Energy & Fuels.* 2015;29(8):5322-5333.

26. Gale TK. *Effects of pyrolysis condition on coal char properties* [PhD Dissertation]. Provo: Chemical Engineering, Brigham Young University; 1994.

27. Smith KL, Smoot LD, Fletcher TH, Pugmire RJ. *The structure and reaction processes of coal*. Provo and Salt Lake City, US: Spring Science + Business Media New York; 1994.

28. Zeng D, Clark M, Gunderson T, Hecker WC, Fletcher TH. Swelling properties and intrinsic reactivities of coal chars produced at elevated pressures and high heating rates. *Proceedings of the Combustion Institute.* 2005;30:2213–2221.

29. Zeng D. *Effects of pressure on coal pyrolysis at high heating rates and char combustion* [PhD Dissertation]. Provo: Department of Chemical Engineering, Brigham Young University; 2005.

30. Yang H, Zhao Y, Wang M, Wang J, Hu H. Study on the evolution of pore structure during subbituminous coal pyrolysis *China National Symposium on Combustion*. Nanjing, China 2017.

31. Zhang K, Li Y, Wang ZH, et al. Pyrolysis behavior of a typical Chinese sub-bituminous Zhundong coal from moderate to high temperatures. *Fuel.* Dec 2016;185:701-708.